

## THE BEHAVIOR OF GAS-LIQUID INTERFACES IN VERTICAL TUBES

GRAHAM B. WALLIS and JING TZONG KUO

The Thayer School of Engineering, Dartmouth College, Hanover, NH 03755, U.S.A.

(Received 29 May 1975)

**Abstract**—Experimental studies of interface behavior when a gas flow, confined in a vertical tube, flows past a stationary body of liquid are presented. Critical conditions necessary for the interface to become unstable or break up are investigated. Specific phenomena studied include: penetration of liquid from a reservoir into the top open end of a vertical tube from which gas is emerging, flow of gas past a liquid ring maintained on the inside wall of the tube, conditions for the support of a “hanging film” on the tube wall, formation of droplets and establishment of a continuous upwards-flowing liquid film. A general mathematical formulation of this problem is presented and used to derive the set of relevant dimensionless parameters. Solutions are obtained to certain simple cases and are shown to be consistent with experiment in the limits in which one or more of the variables exerts negligible influence.

### INTRODUCTION

An important category of gas-liquid two-phase flow is the “separated” flow regime in which the components flow side by side, separated by a continuous interface. A common difficulty with the development of analysis for describing this regime is the problem of deciding what the interface shape is. Until the interface shape is known, detailed analysis of the field equations on either side of it usually cannot be performed. The solution must satisfy suitable kinematic and stress boundary conditions at this interface, so only a limited set of interface shapes is possible. A further complication may arise if stability is considered; the interface may be dynamically unstable and cannot maintain its original shape.

Examples of problems in this class are: interfacial waves in stratified horizontal flow, such as occur in meteorology, the generation of waves by winds over bodies of water, or in pipelines for transporting oil and gas; capillary ripples and roll-waves in vertical annular flow, the instability of falling films under countercurrent gas flow which results in “flooding”, behavior of sheets of water on the windshield of a car under the influence of air flow, the mechanics of coughing, and the penetration of emergency core coolant water into a nuclear reactor, following a possible “loss of coolant accident”, while steam is being evolved.

This paper considers a problem of this type. A vertical gas flow, confined in a tube, flows past a liquid interface which is maintained in a variety of ways (for example, by allowing communication with a reservoir) without there being any net liquid flow. A formal idealised mathematical problem is posed and exact and approximate solutions are presented for simplified “limiting cases”. Interface shapes and stability are studied experimentally for a variety of conditions which are generally more complicated than the situations for which solutions are developed. Emphasis is placed on certain “critical” conditions at which a change in behavior is observed. Key dimensionless groups, derived from the theory, are identified and used to present data obtained by varying some parameters, such as tube diameter and gas flow rate, over a wide range. The data show agreement with theory in the “limiting cases” and the expected qualitative trends in between.

There do not seem to have been many previous studies of these phenomena. Some authors, notably Kutateladze and his co-workers (1958, 1972), have set up similar general field equations, derived a complete set of dimensionless groups and presented some empirical correlations. However, particular solutions supported by both theory and experiment, are rare, e.g. Shearer & Davidson (1965) on wave formation by gas blowing over a viscous falling film. Kuo (1974) has tried using Shearer & Davidson’s approximations for the stationary liquid problem discussed in

this paper but they did not lead to the prediction of a "critical" gas velocity. The various theories of interfacial waves in gas-liquid annular flow (Hewitt & Hall-Taylor 1970) do not agree very well with observations. The most recent work, which stimulated the present investigation, concerned the "hanging film" phenomenon in which liquid on the inner wall of a vertical tube was supported against gravity by upwards gas flow through the tube (Pushkina & Sorokin, 1969; Wallis & Makkenchery, 1974).

#### FORMAL PROBLEM STATEMENT

Figure 1 shows the situation being considered. Gas with density  $\rho_G$  flows over liquid with density  $\rho_L$ . At  $x = +\infty$  the gas velocity is uniform and equal to  $U$  in the negative  $x$ -direction. The gas flow is considered to be inviscid and irrotational. The liquid is considered to be stationary. The flow is confined in a tube of radius  $r_0$ . Cylindrical coordinates  $(r, x)$  are used (sometimes the alternative coordinate  $y = (r_0 - r)$  is employed).

There is a stagnation point at  $y = 0$ ,  $x = x_0$ , where the liquid meets the wall with contact angle  $\beta$ . The pressures of the liquid and gas at this stagnation point are  $p_{0L}$  and  $p_{0G}$ , respectively.

At some point on the interface the liquid and gas pressures are  $p_L$  and  $p_G$  and let the gas speed be  $v$ .

From hydrostatics for the liquid, neglecting its motion, if any (an assumption valid for the ideal limiting cases we will consider later, but requiring examination under different circumstances),

$$p_L = p_{0L} - \rho_L g(x_0 - x). \quad [1]$$

From Bernoulli's equation for the gas,

$$p_G = p_{0G} - \rho_G g(x_0 - x) - \frac{1}{2} \rho_G v^2. \quad [2]$$

Across the interface, due to effect of surface tension  $\sigma$

$$p_L = p_G - \sigma \left\{ \frac{\frac{d^2x}{dy^2}}{\left[1 + \left(\frac{dx}{dy}\right)^2\right]^{3/2}} + \frac{\left|\frac{dx}{dy}\right|}{r \left[1 + \left(\frac{dx}{dy}\right)^2\right]^{1/2}} \right\}. \quad [3]$$

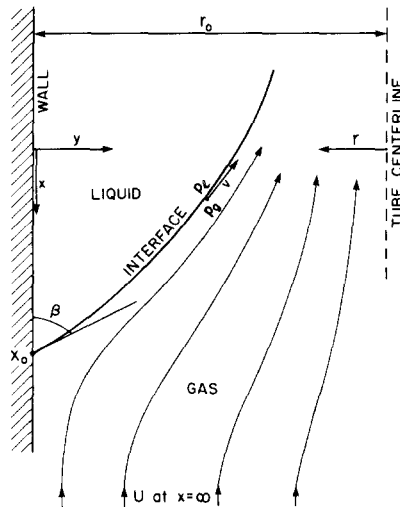


Figure 1. Flow of gas past a liquid interface attached to the wall of a vertical tube.

(For some interface shapes it may be necessary to be careful about the sign of the interfacial curvature.) Combining [1], [2] and [3] we get

$$p_{0G} - p_{0L} = \frac{1}{2} \rho_G v^2 + \sigma \left\{ \frac{\frac{d^2x}{dy^2}}{\left[1 + \left(\frac{dx}{dy}\right)^2\right]^{3/2}} + \frac{\left|\frac{dx}{dy}\right|}{r \left[1 + \left(\frac{dx}{dy}\right)^2\right]^{1/2}} \right\} - g \Delta \rho (x_0 - x) \quad [4]$$

with  $\Delta \rho = (\rho_L - \rho_G)$ .

The problem is to determine an interface shape such that [4] is satisfied everywhere, for given boundary conditions. The term  $p_{0G} - p_{0L}$  is merely a constant, which does not depend on  $x$  or  $y$ , equal to the value of the right hand side at the stagnation point.

Boundary layer growth and eventual "separation" on the interface complicate this problem, but the above approach should be valid near the stagnation point at high enough gas Reynolds numbers.

The gas flow can be described by a velocity potential  $\phi$  and the interface is some suitable curve,  $\psi = \text{constant}$ , where  $\psi$  is the stream function. The magnitude of the velocity everywhere is given by

$$v^2 = \left(\frac{d\phi}{dx}\right)^2 + \left(\frac{d\phi}{dy}\right)^2. \quad [5]$$

Define dimensionless coordinates:

$$x^* = x \sqrt{\left(\frac{\Delta \rho g}{\sigma}\right)}, \quad y^* = y \sqrt{\left(\frac{\Delta \rho g}{\sigma}\right)}, \quad [6]$$

and a dimensionless velocity potential as

$$\phi^* = \frac{\phi}{U} \sqrt{\left(\frac{\Delta \rho g}{\sigma}\right)}. \quad [7]$$

Using [6] and [7] in [4] we get

$$\frac{1}{2} \frac{\rho_G U^2}{\sqrt{(\Delta \rho g \sigma)}} \left[ \left(\frac{d\phi^*}{dx^*}\right)^2 + \left(\frac{d\phi^*}{dy^*}\right)^2 \right] + \frac{\frac{d^2x^*}{dy^{*2}}}{\left\{1 + \left(\frac{dx^*}{dy^*}\right)^2\right\}^{3/2}} + \frac{\left|\frac{dx^*}{dy^*}\right|}{r^* \left[1 + \left(\frac{dx^*}{dy^*}\right)^2\right]^{1/2}} - (x_0^* - x^*) = \text{constant}. \quad [8]$$

The key dimensionless group which emerges from [8] is the Kutateladze number,

$$K = \rho_G^{1/2} U (\Delta \rho g \sigma)^{-1/4}, \quad [9]$$

which could be regarded as a dimensionless gas velocity.

The boundary conditions are

$$\frac{d\phi^*}{dx^*} = 1, \quad \frac{d\phi^*}{dy^*} = 0 \quad \text{at} \quad x^* = \infty, \quad [10]$$

$$\frac{dx^*}{dy^*} = -\cot \beta, \quad r^* = r_0^*, \quad \text{at} \quad x^* = x_0^*, \quad [11]$$

so the other two dimensionless numbers defining the problem are  $\beta$ , the contact angle, and the dimensionless radius

$$r_0^* = r_0 \sqrt{\left(\frac{\Delta\rho g}{\sigma}\right)}, \quad [12]$$

or, alternatively, the dimensionless diameter

$$D^* = 2r_0^* = D \sqrt{\left(\frac{\Delta\rho g}{\sigma}\right)}. \quad [13]$$

The boundary conditions in the negative  $x$  direction have been left vague up to this point. There are numerous possibilities. The liquid could be part of a toroidal ring with given volume. It could be the lower end of a "hanging film" supported above its lower end by drag forces from the gas on interfacial waves. It could be part of a pool of liquid surrounding the upper end of the tube and attempting to penetrate down into it. It could be in communication with a constant pressure liquid reservoir. All of these conditions have been investigated experimentally and will be discussed later in this paper. In all cases we would expect the solution to the problem to depend on  $K$ ,  $D^*$  and  $\beta$ , together with some dimensionless representation of the other boundary conditions (and possibly a weak influence of gas Reynolds number to account for boundary layer and separation effects).

One approach to the problem is to explore the solutions to [8] for different values of  $K$ , given  $D^*$  and  $\beta$ . The evaluation of  $\phi$  and  $\psi$  for the "unknown interface" presents some difficulty. A possible approximate analytical technique is to assume a certain class of interface shapes, containing variable coefficients, such that  $\phi$  and  $\psi$  can be evaluated.  $K^2$  can then be determined from the formula, derived from [8]:

$$K^2 = \frac{x_0^* + \sin^3 \beta (d^2 x^*/dy^{*2})_{x_0} + \cos \beta / r_0^* - x^* - \frac{d^2 x^*/dy^{*2}}{\{1 + (dx^*/dy^*)^2\}^{3/2}} - \frac{dx^*/dy^*}{r^* [1 + (dx^*/dy^*)^2]^{1/2}}}{1/2[(d\phi^*/dx^*)^2 + (d\phi^*/dy^*)^2]}. \quad [14]$$

The coefficients are then adjusted until  $K^2$  is sufficiently "constant" over a selected range. "Unreasonable" assumptions could conceivably lead to negative values of  $K^2$  and would have to be rejected.

#### ANALYSIS

##### Limiting cases

(1) *Large*  $D^*$ ,  $K = 0$ .  $dx^*/dr^* \rightarrow 0$  as  $r^* \rightarrow \infty$ . This corresponds to the case of an extensive sheet of liquid with an interface shape which is uniform in the third dimension (perpendicular to the paper in figure 1). This problem was solved by Bankoff (1958), with the result

$$y^* = \ln \left[ \sqrt{\left(\frac{4}{x^{*2}} - 1\right) + \frac{2}{x^*}} \right] - 2 \sqrt{\left(1 - \frac{x^{*2}}{4}\right)}. \quad [15]$$

Although Bankoff considered liquid spreading over a rough horizontal plate, the solution is valid whatever the orientation of the surface to which the interface is attached as long as the "end conditions" are satisfied. Thus [15] can be used to describe the shape of an interface hanging on the outer lip of a large overfilled tea cup, for example.

(2) *Finite*  $D^*$ ,  $K = 0$ . A computer program was written to solve [8] numerically for the case  $U = 0$ ,  $dx^*/dr^* \rightarrow 0$  as  $r^* \rightarrow \infty$ . A fourth order Runge-Kutta technique was used and it was

checked that the numerical results were indistinguishable from [15] in the limit of large  $D^*$ . A family of curves was generated, as shown in figure 2, by varying the value of the initial surface slope at a large value of  $r^*$ . The curves on the right of this family tend to a limit described by [15] and have an overall dimensionless height from top to bottom equal to 2. The curves which penetrate to smaller values of  $r^*$  have a smaller overall height and tend to be pulled in towards the axis by the effects of a sharper curvature about that axis.

One application of these results is for describing the spreading of a liquid film over the mouth of a sharp-edged hole in a horizontal surface. Let the dimensionless height of the liquid surface above the hole by  $H^*$  at a large distance from the axis. For a given contact angle, the equilibrium value of  $H^*$  decreases as the edge of the liquid approaches the hole. Therefore, if the initial value of  $H^*$  is maintained, the liquid will be drawn to the hole and will hang on the lip, adopting a shape drawn from the set illustrated in figure 3, such that the height of the surface at a large value of  $r^*$  is again  $H^*$ .

The curves in figure 3 are from the same family as those in figure 2. The  $x^*$  origin is merely shifted. For example, figure 2 shows how the curve through the point  $x^* = 1.6$ ,  $r_0^* = 2.6$  can be "attached" to the corner to represent the condition shown in figure 3 with  $H^* = 1.6$ ,  $r_0^* = 2.6$ .

If the radius of the hole is too small there may exist no solution which can fulfill this requirement. This will be so if  $H^*$  and  $r_0^*$  when plotted on figure 2 lie outside the dashed curve describing the maximum possible value of  $H^*$  for a given  $r_0^*$ . In this case the liquid either spills into the hole or is drawn over the hole to "close it off" with a new meniscus forming right across the top of the hole. This sequence of events could be called "critical mechanism I".

An alternative "critical" condition (mechanism II) is reached when the contact angle at the edge of the film, measured from the tube wall (or its extension), reaches the equilibrium value  $\beta$ . This may or may not occur before  $H^*$  achieves the maximum value shown in figure 2, depending on the conditions.

Figure 3 shows a situation in which the liquid first penetrates to the hole when the height,  $H^*$ ,

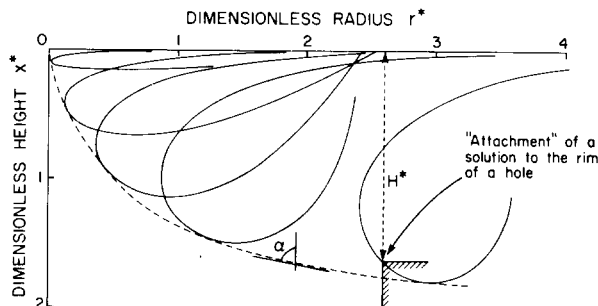


Figure 2. Several computer solutions to [8] with  $U = 0$  and  $dx^*/dr^* \rightarrow 0$  as  $r^* \rightarrow \infty$ .

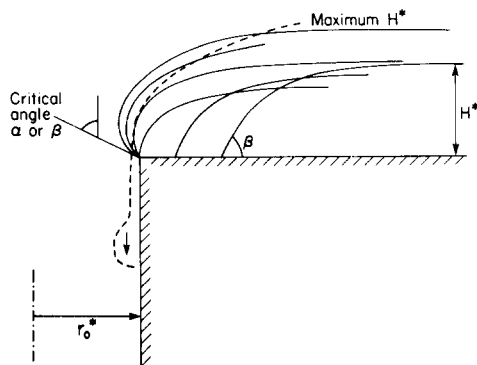


Figure 3. A possible series of shapes for a liquid film spreading into a vertical tube from a horizontal reservoir.

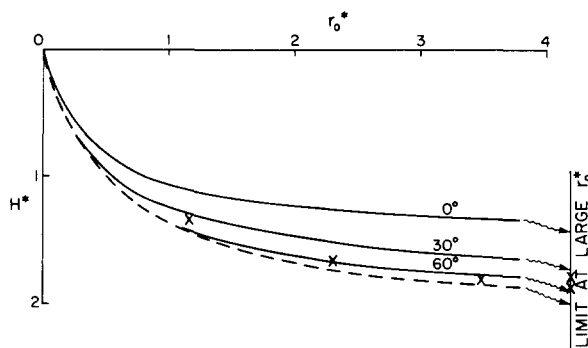


Figure 4a. Relationship between dimensionless tube radius,  $r_0^*$ , and maximum dimensionless free surface height,  $H^*$ , above a sharp-edged circular hole for various values of acute contact angle, with the interface hanging on the lip of the hole. ---- Mechanism I, — Mechanism II, × Data for water on Plexiglas.

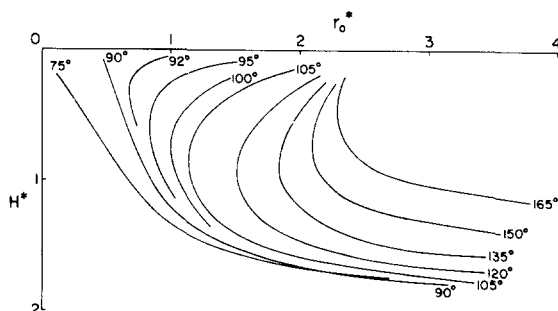


Figure 4b. Relationship between dimensionless tube radius,  $r_0^*$ , and dimensionless free surface height,  $H^*$ , above a circular hole for various values of obtuse contact angle, with the interface hanging on the lip of the hole.

of the surface at large  $r_0^*$  is a little larger than that corresponding to the equilibrium value for a contact angle  $\beta$  measured to the horizontal through the liquid at  $r_0^*$ . If  $H^*$  is increased the surface adopts the sequence of shapes shown in the sketch until the angle of the interface to the vertical at the hole reaches either (1)  $\alpha$ , the angle made between the dashed line in figure 2 and the vertical at the particular value of  $r_0^*$  (Mechanism I) or (2)  $\beta$ , the equilibrium contact angle for liquid about to penetrate downwards into the hole (Mechanism II).

If  $\alpha < \beta$ , Mechanism I occurs first, becoming the dominant mechanism as  $r_0^*$  gets smaller and  $\alpha \rightarrow 0$ .

Figure 4a shows the predicted maximum liquid heights above a sharp-cornered hole as a function of tube radius for several acute contact angles. For a contact angle of  $60^\circ$ , for example, Mechanism I dominates out to about  $r_0^* = 1$  with Mechanism II taking over at larger radii.

Our experiments† with the sharp-edged Plexiglas tube shown in figure 10 gave critical conditions for liquid bridging or penetration of the hole at zero gas flow in several tube sizes as

$r_0^* = 1.16$	$H^* = 1.33$
$r_0^* = 2.32$	$H^* = 1.66$
$r_0^* = 3.5$	$H^* = 1.8$
$r_0^* = 5.81$	$H^* = 1.78-1.86$
$r_0^* = 11$	$H^* = 1.78-1.88$

corresponding to Mechanism II with a contact angle of about  $40^\circ$  to  $60^\circ$  which is near the measured value for water on Plexiglas.

Should the contact angle be obtuse, Mechanism I occurs first at all values of  $r_0^*$ . Figure 4b is a

†Some of these results were obtained by Jim Lay, M.E. candidate at the Thayer School, Dartmouth College.

plot of free surface height  $H^*$  versus tube radius  $r_0^*$  for various values of contact angle. At a given value of  $r_0^*$  there are either two solutions or none for  $H^*$ . The solution giving the lower value of  $H^*$  resembles a squashed doughnut penetrating inwards most of the way to the axis and is most likely highly unstable. The solution corresponding to the higher value of  $H^*$  can presumably only be obtained by passing through the Mechanism I crisis and somehow restricting the liquid inventory so that  $H^*$  can stabilise at a value less than the maximum in figure 2. For each contact angle there is a critical value of  $r_0^*$  below which no solutions at all are possible.

(3) *Large  $D^*$ ,  $K \neq 0, \beta = 90^\circ$ .* If  $D^*$  is large, curvature in the hoop direction can be neglected and the flow regarded as a two-dimensional plane flow. The usual methods of complex variables can be applied by defining

$$z = x + iy \tag{16}$$

and a complex velocity potential

$$w = w[z] = \phi + i\psi. \tag{17}$$

Dimensionless forms consistent with the previous definitions in [6] and [7] are

$$z^* = z \sqrt{\left(\frac{\Delta\rho g}{\sigma}\right)}, \tag{18}$$

$$w^* = \frac{w}{U} \sqrt{\left(\frac{\Delta\rho g}{\sigma}\right)}. \tag{19}$$

Equation [14] becomes

$$K^2 = 2 \left\{ x_0^* + \sin^3 \beta \left(\frac{d^2 x^*}{dy^{*2}}\right)_{x_0} - x^* - \frac{d^2 x^*/dy^{*2}}{[1 + (dx^*/dy^*)^2]^{3/2}} \right\} \left| \frac{dw^*}{dz^*} \right|^{-2}. \tag{20}$$

Various simple flows can be chosen in an attempt to obtain reasonable values for  $K$ . Some, such as flow around a source or around an ellipse are unsuitable since they give monotonically changing values of  $K^2$  as one moves along the interface. A more successful choice of an approximate shape is obtained from the flow around a pair of sources transverse to a uniform flow (figure 5). The ‘‘sources’’ have no physical significance. All that we are doing is constructing a potential flow with the correct overall properties and enough variable parameters to allow approximate fitting of the interface conditions (represented by a constant value of  $K$  in [20]). The

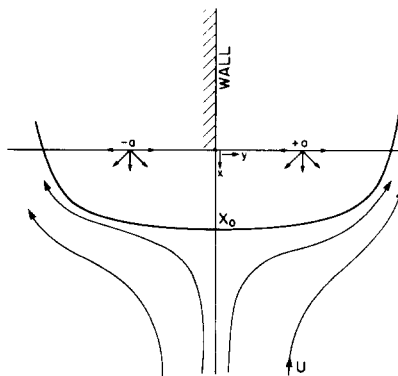


Figure 5. Flow around a pair of sources.

form of the mathematical model which we have chosen restricts us to the particular case  $\beta = 90^\circ$ .

If the sources have “strength”  $A$ , and are located at  $(0, \pm a)$ , the velocity potential describing this flow is

$$w = Uz - A \ln(z^2 + a^2). \quad [21]$$

By increasing “ $a$ ” the interface is made flatter, or even indented, near the stagnation point. Increasing  $A$  “swells up” the enclosed area. The shape is determined entirely by the ratio  $Ua/A$ .

Using the dimensionless scheme described previously we can replace [21] by

$$w^* = z^* - A^* \ln(z^{*2} + a^{*2}) \quad [22]$$

with

$$A^* = \frac{A}{U} \sqrt{\left(\frac{\Delta\rho g}{\sigma}\right)}, \quad a^* = a \sqrt{\left(\frac{\Delta\rho g}{\sigma}\right)}. \quad [23]$$

The dimensionless stream function is

$$\psi^* = y^* - A^* \tan^{-1}\left(\frac{2x^*y^*}{x^{*2} + a^{*2} - y^{*2}}\right) \quad [24]$$

and the interface is given by  $\psi^* = 0$ , or

$$x^{*2} + a^{*2} - y^{*2} = \frac{2x^*y^*}{\tan(y^*/A^*)}. \quad [25]$$

At a given value of  $y^*$ , [25] is a quadratic for  $x^*$  with the physically realistic solution (for  $y^*/A^* < \pi$ )

$$x^* = \frac{y^*}{\tan(y^*/A^*)} + \sqrt{\left(\frac{y^{*2}}{\tan^2(y^*/A^*)} + y^{*2} - a^{*2}\right)}. \quad [26]$$

The stagnation point is at

$$x^* = A^* + \sqrt{A^{*2} - a^{*2}} \quad [27]$$

and the interface cuts the  $y$  axis at

$$x^* = 0, \quad y^* = \pi A^*. \quad [28]$$

The square of the dimensionless velocity is obtained by differentiating [22] and is

$$\left|\frac{dw^*}{dz^*}\right|^2 = \frac{(x^{*2} + a^{*2} - y^{*2} - 2A^*x^*)^2 + (2x^*y^* - 2A^*y^*)^2}{(x^{*2} + a^{*2} - y^{*2})^2 + 4x^{*2}y^{*2}}. \quad [29]$$

The method of solution which was adopted was to solve for the interface using [26] and the velocity using [29] and to calculate the curvature terms in [20] numerically by a finite difference technique over 18 steps in  $y^*$ , starting near the stagnation point and ending short of the  $y^*$  axis (where the computation becomes more tricky). At each point the value of  $K$  was computed. Choosing one value of  $a^*$ ,  $A^*$  was varied until  $K$  remained as constant as possible (usually



within 10% of the mean value) over this interval. The average value of  $K$  for these 18 points was computed and taken as the "best estimate" of  $K$  for that choice of  $a^*$ .  $a^*$  was varied from zero (equivalent to a single source on the axis) up to the point where negative values of  $K^2$  were predicted over part of the interface.

Since the interface shape and the dimensionless velocity are calculated algebraically the only, rather small, influence of the step size is on the accuracy of the differential terms in [20]. Increasing the number of points to 48, for example, gives an increase in the average  $K$  of only 1%; this is more precise than the accuracy with which one can determine the best "fit" to maintain  $K$  approximately constant along the interface.

Over the range  $0.35 < A^* < 2$  the Kutateladze number at the best combination of  $a^*$  and  $A^*$  varied less than 10% (sometimes less than 5%) from its mean value for all of the computed points.

At low values of  $A^*$  and  $K$  deviations became larger and it became impossible to obtain a reasonable fit below about  $A^* = 0.32$  due to the emergence of negative values of  $K^2$ . The explanation for this is that the particular class of solutions chosen cannot provide a good fit near the limit of small  $K$ , where gravity and surface tension forces dominate. (Negative values of  $a^{*2}$  do not lead to reasonable solutions.) Predicted interface shapes for low values of  $K$  are shown in figure 6.

At high values of  $A^*$  it becomes progressively harder to get a good fit. The maximum deviation of  $A^* = 3.46$ ,  $K = 1.77$ , for example, has increased to 20%. As  $A^*$  approaches 4 the deviation rapidly increases to 100% and negative values of  $K^2$  emerge. The interface becomes indented near the stagnation point and the width/height ratio of the enclosed shape increases (figure 7). The predicted value of  $K$  falls off markedly. All of these observations can be interpreted as symptoms of instability of the interface. The exact limit of stable solutions is

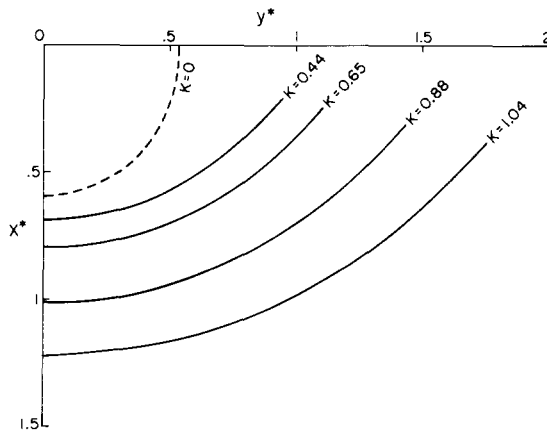


Figure 6. Interface shapes for  $\beta = 90^\circ$  at low values of  $K$ . — predicted from two source model, ---- analytical solution for  $K = 0$ .

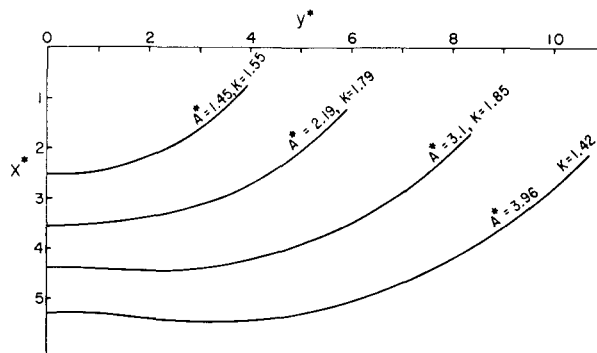


Figure 7. Interface shapes for large values of  $A^*$  and  $K$  with  $\beta = 90^\circ$ .

perhaps not rigorously obtained without a perturbation analysis. However, it would appear that a condition in which the "equilibrium" size of the projection of the liquid into the gas flow increases with a decrease in gas flow rate is grossly unstable as long as excess liquid is available to make up the additional mass enclosed by the interface.

Figure 8 shows the relationship between  $K$  and  $A^*$ . In view of [28],  $A^*$  gives a measure of the size of the liquid projection. The dashed line in figure 8 has been drawn to give a value at  $K = 0$  in agreement with Bankoff's solution. The maximum value of  $K$  is 1.87 and instability would likely be observed in practice at a lower value as a result of interface oscillations causing a jump to unstable conditions near the right hand end of the curve. The maximum value of  $K$  in figure 8 corresponds very closely to the condition  $d^3x^*/dy^3 = 0$  at the stagnation point (i.e. the transition to "reversed curvature" there).

The similar problem of distortion of a large droplet falling in a stationary gas gives an experimental value of  $K \approx 1.41$  at the instability point corresponding to the largest allowable size (Wallis 1974).

The solution developed above was for the special case  $\beta = 90^\circ$ . In general, the critical value of  $K$  in a large pipe would be expected to depend on  $\beta$ .

Though approximate, this mathematical development has been useful for the following purposes: (1) It reveals the key role played by the Kutateladze number and enables an estimate to be made of its critical value. (2) The approach to instability, as the size of the liquid protrusion is increased, is consistent with observation and physical arguments. (3) Future more sophisticated analyses (and experiments) can be compared with these relatively simple predictions.

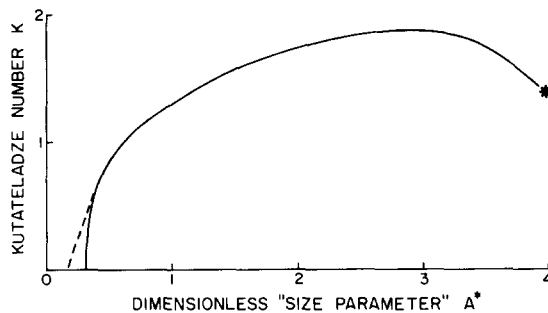


Figure 8. Dependence of  $K$  upon size ( $\beta = 90^\circ$ ) \*—emergence of negative values of  $K^2$  over part of the interface.

### *The general case*

It might be possible to pursue the general solution of the original problem by setting up the velocity potential for flow in a tube as a series of eigenfunctions (Bessel functions in this case) and solving for the coefficients which will enable the boundary and interface conditions to be satisfied. A finite-difference approach to the velocity field, using iteration to get progressively better approximations to the interface shape, could also be tried (Kuo 1974). However, we already have established the important dimensionless groups ( $D^*$ ,  $K$  and  $\beta$ ), and the idea that  $D^*$  is unimportant in large pipes while in small tubes (small  $D^*$ ) surface tension can lead to "critical conditions" (such as bridging) when  $K = 0$ . We therefore chose to pursue an experimental study at this stage, looking at several manifestations of the general phenomena of interest.

### EXPERIMENTS

Three classes of experiment were performed: (1) A liquid film supported above a dry wall region on the inside of a vertical tube under the influence of an upwards air flow (the "Hanging Film" experiment) (figure 9). (2) Penetration of liquid from above into a vertical circular hole under the influence of gas flowing upwards through the hole (figure 10). (3) The behavior of a toroidal liquid ring hanging around the inner wall of a tube as gas is blown upwards through the

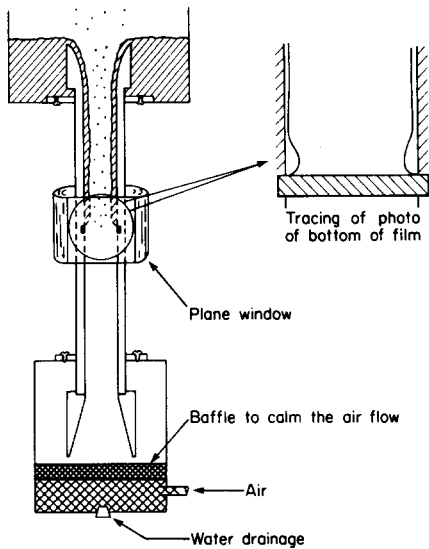


Figure 9. A liquid film supported by upward flow of gas in a vertical tube (not to scale).

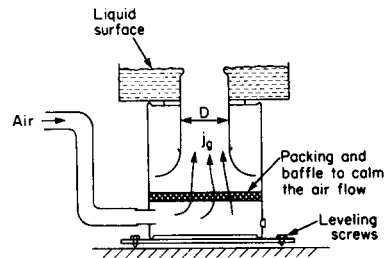


Figure 10. Experimental apparatus for studying the penetration of liquid into large tubes (not to scale).

tube. Two ways of locating this ring were used: (a) insertion of a teflon (a non-wettable plastic) washer into the tube wall (figure 11), (b) splitting the tube so that the ring was supported on the lower corner and water could be supplied through the circumferential slit from a reservoir with a controlled liquid head (figure 12).

Details of the experimental procedures and results, including photographs of the observed interface shapes, are given in the thesis by Kuo (1974). For the purposes of this paper we summarize only the more significant results which have been gathered into figure 15. The lines through the three main sets of data have been drawn freehand but show the expected "limiting behavior" with  $K \rightarrow 0$  at low values of  $D^*$  and  $K \rightarrow$  a constant at high values of  $D^*$ .

(1) *Hanging liquid film*

The hanging film phenomenon has been described previously by Wallis & Makkenchery (1974). Using an apparatus similar to that shown in figure 9 (but without the teflon washer) these authors measured the minimum average gas velocity needed to prevent liquid from penetrating continuously down the wall of a vertical tube which had previously been dried out. Their results

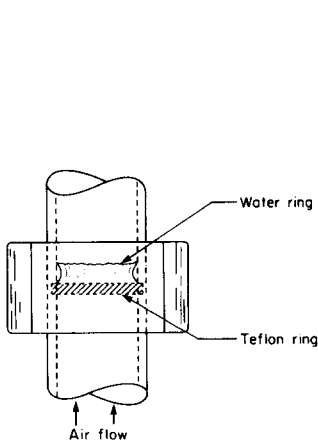
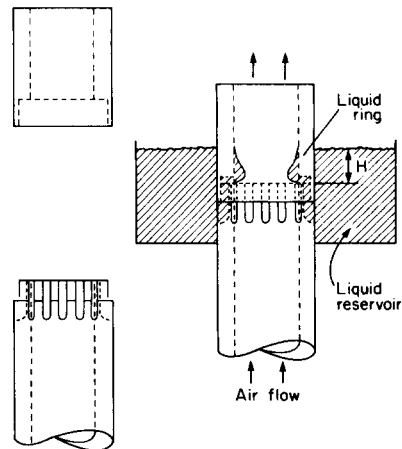


Figure 11. A ring of liquid hanging above a Teflon ring inside a vertical tube.



a. Upper and lower tubes      b. Assembly

Figure 12. Design for the hanging ring experiment.

were presented in terms of a "critical Kutateladze number" as a function of  $D^*$ , with a suggested influence of contact angle, since glass and plastic tubes gave different results. They also discussed an alternative dimensionless form of gas velocity

$$j_g^* = \frac{K}{\sqrt{(D^*)}},$$

which does not contain surface tension as a parameter, and indicated that a constant  $j_g^*$  could provide a reasonable fit to their data at "intermediate" values of  $D^*$ .

We did not repeat this earlier work. However, a limited number of data points were obtained using silicon oil instead of water. The silicon oil has a surface tension of  $2 \times 10^{-2}$  N/m, less than one third that of water, and a density close to water. Its contact angle was very low and it spread rapidly over the plastic surfaces used. The data (figure 15) show partial agreement with earlier results but the value of  $K$  at  $D^* = 42$  is unexpectedly high. In fact, both the water-glass tube, silicon oil-plastic tube data fit a " $j_g^* = \text{constant}$ " hypothesis quite well.

We also took photographs of the lower end of the film hanging in the apparatus shown in figure 9 for the conditions represented by the \* in figure 15. The picture was used to trace the outline shown in figure 9 indicating that the bottom of the film consists of a large "standing wave" substantially thicker than the oscillating film above it.

### (2) Penetration of liquid into a vertical hole

Figure 10 shows the essence of the apparatus. Two inlet nozzle designs were used, a well-rounded one, as shown, and a conical one like the one in figure 9. The tube diameters tested were

$D$ (mm)	6.4	19	31.2	38.2	63.5	113	145
$D^*$	2.4	7.0	11.5	14.0	23.3	42.0	53.2

Air was supplied to the tube via the nozzle from a large plenum chamber equipped with packing for removing turbulence. The water level was measured with a micrometer. The top of the tube was carefully machined flat and leveled.

The behavior of the liquid meniscus at the top of the tube was observed as a function of  $H^*$  and  $K$ . Two "critical" phenomena were noticed: (1) At a low value of  $K$ , increasing  $H^*$  led eventually to liquid penetration over the lip of the tube and running of liquid down the inner wall. As  $K$  was increased the corresponding critical value of  $H^*$  also increased. (2) At high values of  $K$ , increasing  $H^*$  led to the pulling of large liquid sheets outwards, more or less horizontally from the film, and the ejection of drops in a "crown" shape upwards from the edge of the tube. No liquid penetration of the tube occurred. As  $K$  was increased the corresponding critical value of  $H^*$  decreased.

Typical results are shown in figure 13.

The value of  $K$  at the transition between the two above mechanisms was evaluated. This is the "critical" value of  $K$  above which no penetration of the tube occurred, no matter how large the value of  $H^*$ .

These critical values of  $K$  are shown as a function of  $D^*$  in figure 15. They show a trend very similar to the results of the hanging film experiment. The values of  $K$  are perhaps slightly higher in the hanging film case because waves on the film lead to oscillations of the interface and a higher gas velocity is needed to support a jiggling liquid ring than is needed to support a relatively stationary one (there being some downwards liquid motion to be counteracted at times in the former case).

### (3) Liquid ring formed at a horizontal split in the tube

Figure 12 shows the apparatus. Two pieces of tube were machined, grooved, fit together and

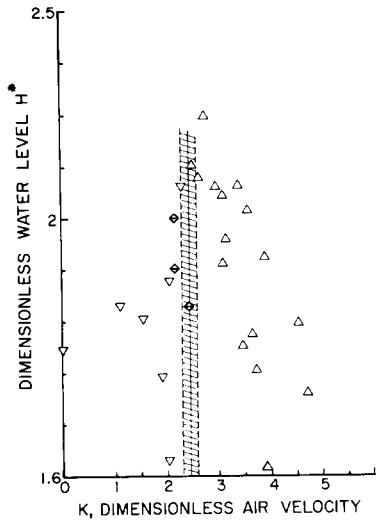


Figure 13. Relationship between water level and critical air velocity in the liquid penetration experiment  $D = 63.5$  mm,  $D^* = 23.3$ . ▽—water runs down the tube, Δ—water is ejected upwards.

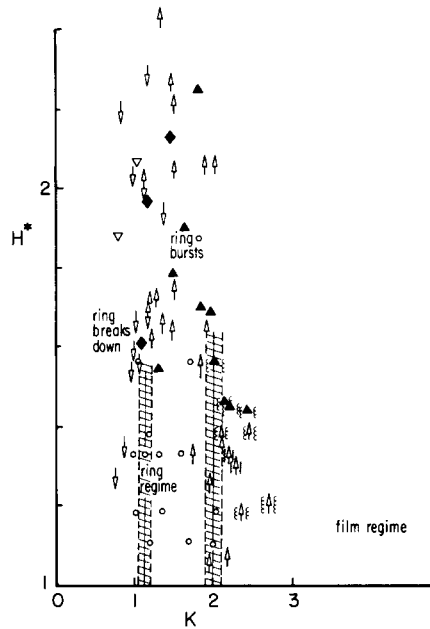


Figure 14. The behavior of a water ring for different air velocities and water depth.  $D = 31.2$  mm,  $D^* = 11.5$ . (See table 1 for description of symbols).

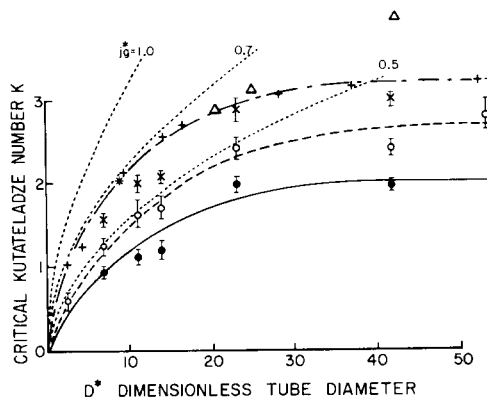



Figure 15.

+ , Hanging film result of Wallis & Makkenchery; \* , Teflon ring experiment; Δ , Minimum air velocity to support a silicone oil film; O , Critical air velocity above which water will not penetrate a hole; × , Minimum air velocity for upwards flowing water film formation from a slit in communication with a reservoir; ● , Minimum air velocity for the formation of droplets from a water ring; .....  $j_r^* = \text{constant}$ . (Pushkina & Sorokin observed a critical  $K$  of 3.2.) Error bars denote uncertainty in estimating the transition velocities.

surrounded by an annular reservoir into which liquid was supplied. A liquid ring formed in the tube pivoted about the upper edge of the lower tube. Air was blown vertically upwards through the tube and the behavior of the ring was studied for various values of  $H^*$  and  $K$ .

As  $H^*$  was increased, three modes of “breakdown” of the ring were observed, depending on the value of  $K$ . (a) At low values of  $K$  the liquid simply ran down the tube, if too much were added to the reservoir. (b) At intermediate values, “tongues” of liquid were pulled out almost horizontally from the ring, broken into droplets and blown up the tube and into the surrounding room; this is the “bursting” of the ring indicated in figure 14. (c) At high values of  $K$  the ring extended upwards along the wall to form a continuous climbing film on the tube above the entrance slot.

Table 1. Symbols for the hanging ring experiment (figure 14)

		$\text{J} \cup$ : Rounded nozzle inlet	$/ \setminus$ : Conical nozzle inlet
Air inlet	Symbol	Description	
$\text{J} \cup$ $/ \setminus$	$\nabla$ $\downarrow$	Ring breaks down, liquid snakes down along the wall.	
$\text{J} \cup$ $/ \setminus$	$\blacktriangle$ $\uparrow$	Ring breaks, droplets are blown out of the tube into the surrounding room.	
$\text{J} \cup$ $/ \setminus$	$\blacklozenge$ $\updownarrow$	Ring breaks, a rough liquid film runs downwards and droplets are entrained in the gas core and are blown upwards.	
$\text{J} \cup$ $/ \setminus$	$\{\blacktriangle\}$ $\{\uparrow\}$	A ring of liquid can hardly be formed before it is pushed upwards into a "climbing film". The film is rough at low gas flow rates and smoother at high gas flow rates. At high gas flow rates, a train of waves moves upwards on its surface.	
		Transition regions	
	$\circ$	Stable ring.	

Typical results are shown in figure 14 with a description of the phenomena summarised in table 1. Results for both a conical and "well-rounded" air nozzle at the bottom of the tube are shown.

These two "critical" values of  $K$  are plotted in figure 15 and are seen to display characteristics similar to the former experimental results, tending to a limiting value of  $K$  at large values of  $D^*$ .

#### DISCUSSION

The various experiments described in this paper all show similar characteristics which are generally both qualitatively and quantitatively consistent with theoretical expectations, over the range of parameters which have been investigated. Though the resulting phenomena may vary in detail, the behavior of a gas-liquid interface on the inner wall of a vertical tube appears to depend on various "critical" values of the Kutateladze number, all of which approach zero in small tubes and tend to a limit, roughly consistent with our approximate theory which predicts  $K \rightarrow 1.87$  in large tubes for the special case of  $\beta = 90^\circ$ . Over a range of intermediate diameters the alternative dimensionless representation of the gas velocity  $j_g^*$  is approximately constant which may explain why some authors have successfully correlated data using this parameter.

For completeness it would be desirable to perform similar experiments in which more physical properties, such as surface tension, gas density and contact angle were systematically varied. A more complete theory could also be sought. However, this paper has established a basic picture of the phenomena, the important dimensionless groups and a sufficient blend of theory and experiment to suggest that further work is likely to be consistent with the results which we have reported.

One question which we did not answer adequately was, "what happens if a large mass of liquid is present on the wall of a large tube?" The trend to a constant value of  $K$  at large values of  $D^*$  implies that the liquid film thickness is scaled by surface tension and the "characteristic length" is  $\sqrt{(\sigma/g\Delta\rho)}$  rather than  $D$ . What if, somehow, a liquid ring with dimension comparable

with  $D$  is established? We attempted to do this by pouring a bucketful of water directly into the top of our largest tube while air was emerging at a  $K$  of around 3.5. The water all blew out in our faces. However, we are not convinced that a way of introducing a large amount of liquid, perhaps asymmetrically with some initial downward momentum, could not be found which would allow penetration above the critical values of  $K$  reported here.

#### CONCLUSIONS

This paper has described several changes in flow regime (qualitative behavior) which occur at some "critical velocity" when gas is blown past a continuous liquid film hanging on the inside of a vertical tube. The behavior appears to be mostly described by three independent dimensionless groups;

Kutateladze number

$$K = U\rho_g^{1/2}[\sigma g(\rho_L - \rho_G)]^{-1/4},$$

Dimensionless diameter

$$D^* = D \left[ \frac{g(\rho_L - \rho_G)}{\sigma} \right]^{1/2},$$

Contact angle

$$\beta.$$

The first two groups can be combined to give an alternative dimensionless representation of the gas velocity

$$j_G^* = U\rho_g^{1/2}[gD(\rho_L - \rho_G)]^{-1/2}.$$

In sufficiently small tubes ( $D^* \leq 2$ ) liquid bridging occurs. In large tubes ( $D^* \geq 30$ ) the maximum amount of liquid which can be supported against gravity occurs at a constant value of  $K$  in the range 1.8–3.2, depending on the details of the experiment. At intermediate values of  $D^*$  a constant value of  $j_G^*$  will correlate the transition fairly well.

Further experiments in which some of the parameters remaining constant in this study were varied would be desirable in order to establish a general correlation of these phenomena.

*Acknowledgement*—This work was supported in part by the National Science Foundation; Grant GK-35624.

#### REFERENCES

- BANKOFF, S. G. 1958 Entrapment of gas in the spreading of a liquid over a rough surface. *A.I.Ch.E. Jl* **4**, 24–26.
- HEWITT, G. F. & HALL-TAYLOR, N. S. 1970 *Annular Two-Phase Flow*. Chapter 6. Pergamon Press, Oxford.
- KUO, J. T. 1974 The behavior of gas-liquid interfaces in vertical tubes, M.S. Thesis, Dartmouth College, Hanover, NH 03755.
- KUTATELADZE, S. S. & STYRIKOVICH, M. A. 1958 *Hydraulics of Gas-Liquid Systems*, Moscow. (Wright Field Translation F-TS-9814/V).
- KUTATELADZE, S. S. 1972 Elements of the hydrodynamics of gas-liquid systems. *J. Fluid Mech.—Soviet Res.* **1**, 29–50.
- PUSHKINA, O. L. & SOROKIN, YU. L. 1969 Breakdown of liquid film motion in vertical tubes. *J. Heat Transfer—Soviet Res.* **1**, 56–64.

- SHEARER, C. J. & DAVIDSON, J. F. 1965 The investigation of a standing wave due to gas blowing upwards over a liquid film; its relation to flooding in a wetted-wall column. *J. Fluid Mech.* **22**, 321–335.
- WALLIS, G. B. 1974 The terminal speed of single drops or bubbles in an infinite medium. *Int. J. Multiphase Flow* **1**, 491–511.
- WALLIS, G. B. & MAKKENCHERY, S. 1974 The hanging film phenomenon in vertical annular two phase flow, *J. Fluids Engng* **98**, 297–298.